A&A 419, 941–948 (2004)
DOI: 10.1051/0004-6361:20040098

Astronomy & Astrophysics

Density waves in the shearing sheet

IV. Interaction with a live dark halo

B. Fuchs⋆

Astronomisches Rechen-Institut, Mönchhofstrasse 12–14, 69120 Heidelberg, Germany

Received 2 June 2003 / Accepted 19 February 2004

Abstract. It is shown that if the self-gravitating shearing sheet, a model of a patch of a galactic disk, is embedded in a live dark halo, this has a strong effect on the dynamics of density waves in the sheet. I describe how the density waves and the halo interact via halo particles either on orbits in resonance with the wave or on non-resonant orbits. Contrary to expectation the presence of the halo leads to a very considerable enhancement of the amplitudes of the density waves in the shearing sheet. This effect appears to be the equivalent of the recently reported enhanced growth of bars in numerically simulated stellar disks embedded in live dark halos. Finally I discuss the transfer of linear momentum from a density wave in the sheet to the halo and show that it is mediated only by halo particles on resonant orbits.

Key words. galaxies: kinematics and dynamics – galaxies: spiral

1. Introduction

The shearing sheet (Goldreich & Lynden-Bell 1965; Julian & Toomre 1966) model has been developed as a tool to study the dynamics of galactic disks and is particularly well suited to describe theoretically the dynamical mechanisms responsible for the formation of spiral arms. For the sake of simplicity the model describes only the dynamics of a patch of a galactic disk. It is assumed to be infinitesimally thin and its radial size is assumed to be much smaller than the disk. Polar coordinates can be therefore rectified to pseudo-Cartesian coordinates and the velocity field of the differential rotation of the disk can be approximated by a linear shear flow. These simplifications allow an analytical treatment of the problem, which helps to clarify the underlying physical processes operating in the disk.

In the present paper of this series I discuss the dynamical effects if the shearing sheet is immersed in a live dark halo. Dark halos are usually thought to stabilize galactic disks against non-axisymmetric instabilities. This was first proposed by Ostriker & Peebles (1973) on the basis of – low-resolution – numerical simulations. Their physical argument was that the presence of a dark halo reduces the destabilizing self-gravity of the disks. Doubts about an entirely passive role of dark halos were raised by Toomre (1977), but he (Toomre 1981) also pointed out that a dense core of a dark halo may cut the feed-back loop of the corotation amplifier of bars or spiral density waves and suppress thus their growth. Recent high-resolution numerical simulations by Athanassoula (2002, 2003), also inherent in the work of Debattista & Sellwood (2000), have shown that quite the reverse, a *destabilization* of disks immersed in dark halos, actually might be true. Athanassoula (2002) demonstrated clearly that much stronger bars grow in the simulations if the disk is embedded in a live dark halo instead of a static halo potential. This is attributed to angular momentum transfer from the bar to the halo via halo particles on resonant orbits. Angular momentum exchange between disk and halo has been addressed since the pioneering work of Weinberg (1985) in many studies theoretically or by numerical simulations and I refer to Athanassoula (2003) for an overview of the literature. Toomre (1981) has shown how the bar instability can be understood as an interference of spiral density waves in a resonance cavity between the corotation amplifier and an inner reflector (cf. also Fuchs 2004). Thus it is to be expected that a live dark halo will be also responsive to spiral density waves and develop wakes, which I investigate here using the shearing sheet model.

⋆ e-mail: fuchs@ari.uni-heidelberg.de

2. Boltzmann equations

The evolution of the distribution function of the disk stars in phase space is described by the linearized 4-dimensional Boltzmann equation

$$\frac{\partial f_{\rm d1}}{\partial t} + u\frac{\partial f_{\rm d1}}{\partial x} + v\frac{\partial f_{\rm d1}}{\partial y} - \frac{\partial \Phi_{\rm d0}+\Phi_{\rm h0}}{\partial x}\frac{\partial f_{\rm d1}}{\partial u} - \frac{\partial \Phi_{\rm d0}+\Phi_{\rm h0}}{\partial y}\frac{\partial f_{\rm d1}}{\partial v} - \frac{\partial \Phi_{\rm d1}+\Phi_{\rm h1}}{\partial x}\frac{\partial f_{\rm d0}}{\partial u} - \frac{\partial \Phi_{\rm d1}+\Phi_{\rm h1}}{\partial y}\frac{\partial f_{\rm d0}}{\partial v} = 0, \quad (1)$$

where (x, y) denote spatial coordinates with y pointing in the direction of galactic rotation and (u, v) are the corresponding velocity components, respectively. Equation (1) has been derived

from the general 6-dimensional Boltzmann equation assuming delta-function like dependencies of the distribution function on the vertical z coordinate and the vertical w velocity component, respectively, and integrating the Boltzmann equation with respect to them. A perturbation Ansatz of the form

$$f_\mathrm{d} = f_\mathrm{d0} + f_\mathrm{d1},\ \Phi_\mathrm{d} = \Phi_\mathrm{d0} + \Phi_\mathrm{d1},\ \Phi_\mathrm{h} = \Phi_\mathrm{h0} + \Phi_\mathrm{h1} \tag{2}$$

is chosen for the distribution function of the disk stars and the gravitational potentials of the disk and the halo, respectively, and the Boltzmann Eq. (1) has been linearized accordingly.

Similarly the linearized Boltzmann equation for the halo particles can be written as

$$\begin{aligned}&\frac{\partial f_\mathrm{h1}}{\partial t} + u\frac{\partial f_\mathrm{h1}}{\partial x} + v\frac{\partial f_\mathrm{h1}}{\partial y} + w\frac{\partial f_\mathrm{h1}}{\partial z}\\ &\quad -\frac{\partial \Phi_\mathrm{d0}+\Phi_\mathrm{h0}}{\partial x}\frac{\partial f_\mathrm{h1}}{\partial u} - \frac{\partial \Phi_\mathrm{d0}+\Phi_\mathrm{h0}}{\partial y}\frac{\partial f_\mathrm{h1}}{\partial v}\\ &\quad -\frac{\partial \Phi_\mathrm{d0}+\Phi_\mathrm{h0}}{\partial z}\frac{\partial f_\mathrm{h1}}{\partial w} - \frac{\partial \Phi_\mathrm{h1}+\Phi_\mathrm{d1}}{\partial x}\frac{\partial f_\mathrm{h0}}{\partial u}\\ &\quad -\frac{\partial \Phi_\mathrm{h1}+\Phi_\mathrm{d1}}{\partial y}\frac{\partial f_\mathrm{h0}}{\partial v} - \frac{\partial \Phi_\mathrm{h1}+\Phi_\mathrm{d1}}{\partial z}\frac{\partial f_\mathrm{h0}}{\partial w} = 0.\end{aligned} \tag{3}$$

The choice of the dark halo model is lead by the following considerations. One of the deeper reasons for the success of the infinite shearing sheet model to describe spiral density waves realistically is the rapid convergence of the Poisson integral in self-gravitating disks (Julian & Toomre 1966). Consider, for example, the potential of a sinusoidal density perturbation

$$\Phi(x,y) = -G\int_{-\infty}^{\infty}\mathrm{d}x'\int_{-\infty}^{\infty}\mathrm{d}y'\frac{\Sigma_{10}\sin(kx')}{\sqrt{(x-x')^2+(y-y')^2}}, \tag{4}$$

where G denotes the constant of gravitation. At $x = 0$

$$\begin{aligned}\Phi &= -4G\Sigma_{10}\sin(kx)\lim_{x_\mathrm{L}\to\infty}\frac{\mathrm{Si}(kx_\mathrm{L})}{k}\\ &= -\frac{2\pi G\Sigma_{10}\sin(kx)}{k}.\end{aligned} \tag{5}$$

The sine integral in Eq. (5) converges so rapidly that it reaches at $kx_\mathrm{L} = \frac{\pi}{2}$ already at 87% of its asymptotic value. Thus the "effective range" of gravity is about only a quarter of a wave length. The shearing sheet models effectively patches of galactic disks of such size. The wave lengths of density waves are of the order of the critical wave length (Julian & Toomre 1966)

$$\lambda_\mathrm{crit} = \frac{4\pi^2 G\Sigma_\mathrm{d}}{\kappa^2}, \tag{6}$$

where κ denotes the epicyclic frequency of the stellar orbits and Σ_d is the surface density of the sheet. In the solar neighbourhood in the Milky Way, for instance, the critical wave length is $\lambda_\mathrm{crit} = 5$ kpc. Thus it is reasonable to neglect over such length scales, like in the shearing sheet model, the curvature of the mean circular orbits of the stars around the galactic center or the gradient of the surface density. The curvature of the stellar orbits due to the epicyclic motions of the stars, on the other hand, cannot be neglected and is indeed not neglected in the shearing sheet model. The radial size of an epicycle is approximately given by σ_u/κ, where σ_u denotes the radial velocity dispersion of the stars, and the ratio of epicycle size and critical wave length is given by

$$\frac{\sigma_\mathrm{u}}{\kappa\lambda_\mathrm{crit}} = 0.085Q \tag{7}$$

in terms of the Toomre stability parameter Q (Toomre 1964) which is typically of the order of 1 to 2. Concurrent to these approximations I assume a dark halo which is homogeneous in its unperturbed state. Accordingly the curvature of the unperturbed orbits of the halo particles is neglected on the scales considered here and the particles are assumed to be on straight-line orbits. The equations of motion of the halo particles are the characteristics of the Boltzmann equation. In a homogeneous halo $\ddot{\boldsymbol{x}} = \nabla(\Phi_\mathrm{d0}+\Phi_\mathrm{h0}) = 0$, and in accordance with this assumption I neglect the force terms $\nabla\Phi_\mathrm{d0}$ and $\nabla\Phi_\mathrm{h0}$ in the Boltzmann Eq. (3). This simplifies its solution considerably. The disadvantage of such a model is that there are no higher-order resonances of the orbits of the halo particles with the density waves as described by Weinberg (1985) or observed in the high-resolution simulations by Athanassoula (2002, 2003). However their effect was shown to be much less important than the main resonances of the particles with the density waves, which are properly described in the present model.

3. Halo dynamics

The Boltzmann Eq. (3) can be viewed as a linear partial differential equation for the perturbation of the distribution function of the halo particles, f_h1, with inhomogeneities depending on the perturbations of the gravitational potentials of the disk and the halo, $\nabla\Phi_\mathrm{d1}$ and $\nabla\Phi_\mathrm{h1}$, respectively. Thus the equation can be solved for the disk and halo inhomogeneities separately and the solutions combined afterwards by superposition.

3.1. Jeans instability of the halo

I consider first that part of the Boltzmann Eq. (3)

$$\begin{aligned}&\frac{\partial f_\mathrm{h1}}{\partial t} + u\frac{\partial f_\mathrm{h1}}{\partial x} + v\frac{\partial f_\mathrm{h1}}{\partial y} + w\frac{\partial f_\mathrm{h1}}{\partial z}\\ &\quad -\frac{\partial \Phi_\mathrm{h1}}{\partial x}\frac{\partial f_\mathrm{h0}}{\partial u} - \frac{\partial \Phi_\mathrm{h1}}{\partial y}\frac{\partial f_\mathrm{h0}}{\partial v} - \frac{\partial \Phi_\mathrm{h1}}{\partial z}\frac{\partial f_\mathrm{h0}}{\partial w} = 0.\end{aligned} \tag{8}$$

Equation (8) is Fourier transformed with respect to time and spatial coordinates and I consider in the following Fourier terms

$$f_{\mathrm{h}\boldsymbol{k},\omega},\ \Phi_{\mathrm{h}\boldsymbol{k},\omega}\times \mathrm{e}^{i(\omega t+(\boldsymbol{k},\boldsymbol{x}))} \tag{9}$$

with frequency ω and wave vector $\boldsymbol{k}$. If orthogonal spatial coordinates ξ, η, and ζ with ξ parallel to the wave vector $\boldsymbol{k}$ are introduced, Eq. (8) takes the form

$$i\omega f_{\mathrm{h}\boldsymbol{k}} + \upsilon ik f_{\mathrm{h}\boldsymbol{k}} - ik\Phi_{\mathrm{h}\boldsymbol{k}}\frac{\partial f_\mathrm{h0}}{\partial \upsilon} = 0, \tag{10}$$

where $k = |\boldsymbol{k}|$ and υ denotes the velocity component parallel to the ξ-axis. Equation (10) can be immediately integrated with respect to the velocity components perpendicular to $\boldsymbol{k}$.

Adopting for the background distribution function a Gaussian distribution, $f_{\rm h0} = \frac{\rho_{\rm b}}{\sqrt{2\pi}\sigma_{\rm h}} \exp -\frac{\upsilon^2}{2\sigma_{\rm h}^2}$, the solution of Eq. (10) is given by

$$f_{{\rm h}\boldsymbol{k}} = -\Phi_{{\rm h}\boldsymbol{k}} \frac{\upsilon}{\sigma_{\rm h}^2} \frac{k}{\omega + k\upsilon} \frac{\rho_{\rm b}}{\sqrt{2\pi}\sigma_{\rm h}} \exp -\frac{\upsilon^2}{2\sigma_{\rm h}^2}. \tag{11}$$

The corresponding Fourier coefficient of the density perturbation of the halo particles is

$$\rho_{{\rm h}\boldsymbol{k}} = -\Phi_{{\rm h}\boldsymbol{k}} \frac{\rho_{\rm b}}{\sqrt{2\pi}\sigma_{\rm h}^3} \int_{-\infty}^{\infty} {\rm d}\upsilon \frac{\upsilon}{\frac{\omega}{k} + \upsilon} \exp -\frac{\upsilon^2}{2\sigma_{\rm h}^2}. \tag{12}$$

The perturbations of the halo are supposed to be self-gravitating and the gravitational potential has to solve the Poisson equation

$$\left\{\frac{\partial^2}{\partial x^2} + \frac{\partial^2}{\partial y^2} + \frac{\partial^2}{\partial z^2}\right\} \Phi_{{\rm h}\boldsymbol{k}} {\rm e}^{i(\boldsymbol{k},\boldsymbol{x})} = -k^2 \Phi_{{\rm h}\boldsymbol{k}} {\rm e}^{i(\boldsymbol{k},\boldsymbol{x})} = 4\pi G \rho_{{\rm h}\boldsymbol{k}} {\rm e}^{i(\boldsymbol{k},\boldsymbol{x})}. \tag{13}$$

Combining Eqs. (12) and (13) leads to the dispersion relation

$$k^2 = \frac{4\pi G \rho_{\rm b}}{\sqrt{2\pi}\sigma_{\rm h}^3} \int_{-\infty}^{\infty} {\rm d}\upsilon \frac{\upsilon}{\frac{\omega}{k} + \upsilon} \exp -\frac{\upsilon^2}{2\sigma_{\rm h}^2}, \tag{14}$$

which is well known from plasma physics (cf. Kegel 1998). Indeed, the dispersion relation (14) describes simply the Jeans collapse of the halo. From the imaginary part of Eq. (14) one concludes $\Re\omega = 0$ and using formula 3.466 of Gradshteyn & Ryzhik (2000) one obtains from its real part the dispersion relation

$$k^2 = \frac{4\pi G \rho_{\rm b}}{\sigma_{\rm h}^3} \left\{\frac{\sigma_{\rm h}}{2} - \sqrt{\frac{\pi}{2}} \left|\frac{\Im\omega}{k}\right| {\rm e}^{\frac{(\Im\omega)^2}{2k^2\sigma_{\rm h}^2}} {\rm erfc}\left(\frac{\Im\omega}{\sqrt{2}k\sigma_{\rm h}}\right)\right\}, \tag{15}$$

where erfc denotes the complementary error function. As is well known perturbations will grow on length scales larger than the Jeans length $\sqrt{\pi\sigma_{\rm h}^2/G\rho_{\rm b}}$. However, dark halos are thought to be dynamically hot systems and their Jeans lengths will be of the order of the size of the halos themselves. Thus this part of the solution of the Boltzmann Eq. (3) is uninteresting in the present context and will be not considered in the following.

3.2. Response of the halo to a density wave in the disk

I concentrate now on the remaining part of the Boltzmann Eq. (3),

$$\frac{\partial f_{\rm h1}}{\partial t} + u\frac{\partial f_{\rm h1}}{\partial x} + v\frac{\partial f_{\rm h1}}{\partial y} + w\frac{\partial f_{\rm h1}}{\partial z} - \frac{\partial \Phi_{\rm d1}}{\partial x}\frac{\partial f_{\rm h0}}{\partial u} - \frac{\partial \Phi_{\rm d1}}{\partial y}\frac{\partial f_{\rm h0}}{\partial v} - \frac{\partial \Phi_{\rm d1}}{\partial z}\frac{\partial f_{\rm h0}}{\partial w} = 0, \tag{16}$$

which describes the halo response to a perturbation in the disk. If the gravitational potential perturbation of the disk is Fourier expanded the Fourier terms have the form (cf. Eq. (33) of Fuchs 2001)

$$\Phi_{{\rm d}\boldsymbol{k}_\parallel} {\rm e}^{i(k_x x + k_y y) - k_\parallel |z|} \tag{17}$$

with $k_\parallel = |\boldsymbol{k}_\parallel| = \sqrt{k_x^2 + k_y^2}$. This can be converted to the form as in Eq. (9) by introducing Fourier coefficients

$$\Phi_{{\rm d}\boldsymbol{k}} = \frac{1}{2\pi} \int_{-\infty}^{\infty} {\rm d}z \Phi_{{\rm d}\boldsymbol{k}_\parallel} {\rm e}^{-ik_z z - k_\parallel |z|} = \frac{1}{\pi} \frac{k_\parallel}{k_\parallel^2 + k_z^2} \Phi_{{\rm d}\boldsymbol{k}_\parallel}. \tag{18}$$

Note that the coordinate y, which is defined in the reference system of the disk, is related to the y coordinate in the reference system of the halo due to the motion of the center of the shearing sheet as

$$y \to y - r_0\Omega_0 t. \tag{19}$$

Fourier transforming the distribution function of the halo particles as $f_{\rm h1} = \int {\rm d}^3k f_{{\rm h}\boldsymbol{k}} \exp i(\boldsymbol{k},\boldsymbol{x})$ and changing again to ξ, η, ζ coordinates and the corresponding velocity components the Boltzmann Eq. (16) takes the form

$$\frac{\partial f_{{\rm h}\boldsymbol{k}}}{\partial t} + \upsilon i k f_{{\rm h}\boldsymbol{k}} + ik\Phi_{{\rm d}\boldsymbol{k}} \frac{\upsilon}{\sigma_{\rm h}^2} f_{\rm h0} {\rm e}^{i(\omega - k_y r_0\Omega_0)t} = 0, \tag{20}$$

where $k = \sqrt{k_\parallel^2 + k_z^2}$. Equation (20) has been integrated with respect to the velocity components perpendicular to the ξ-axis. Assuming again a Gaussian velocity distribution for the halo particles it can be solved straightforward as

$$f_{{\rm h}\boldsymbol{k}} = -k\Phi_{{\rm d}\boldsymbol{k}} \frac{\upsilon}{\sigma_{\rm h}^2} \frac{{\rm e}^{i(\omega - k_y r_0\Omega_0)t}}{\omega - k_y r_0\Omega_0 + k\upsilon} \frac{\rho_{\rm b}}{\sqrt{2\pi}\sigma_{\rm h}} \exp -\frac{\upsilon^2}{2\sigma_{\rm h}^2}. \tag{21}$$

The corresponding Fourier term of the density perturbation of the halo particles is given by

$$\rho_{{\rm h}\boldsymbol{k}} = -\Phi_{{\rm d}\boldsymbol{k}} \frac{\rho_{\rm b}}{\sqrt{2\pi}\sigma_{\rm h}^3} \int_{-\infty}^{\infty} {\rm d}\upsilon \frac{\upsilon {\rm e}^{-\frac{\upsilon^2}{2\sigma_{\rm h}^2}}}{\frac{\omega}{k} - \frac{k_y r_0\Omega_0}{k} + \upsilon}, \tag{22}$$

where the time-dependent term has been split off and is written no longer explicitely. Next the gravitational potential associated with this density distribution is calculated from the Poisson equation,

$$-k^2 \Phi_{{\rm h}\boldsymbol{k}} = 4\pi G \rho_{{\rm h}\boldsymbol{k}}, \tag{23}$$

resulting in

$$\Phi_{{\rm h}\boldsymbol{k}} = \Phi_{{\rm d}\boldsymbol{k}} \frac{4\pi G \rho_{\rm b}}{\sqrt{2\pi}\sigma_{\rm h}^3} \frac{1}{k^2} \int_{-\infty}^{\infty} {\rm d}\upsilon \frac{\upsilon {\rm e}^{-\frac{\upsilon^2}{2\sigma_{\rm h}^2}}}{\frac{\omega}{k} - \frac{k_y r_0\Omega_0}{k} + \upsilon}. \tag{24}$$

The integral on the rhs of Eq. (24) is not trivial and has to be evaluated as a Cauchy principal value and the pole contribution at $\upsilon = -\frac{\omega}{k} + \frac{k_y r_0\Omega_0}{k}$, where the halo particles travel at velocities in resonance with the Doppler-shifted phase velocity of the wave. Following the method of Kegel (1998) I obtain for the principal value of the integral

$$\Phi_{{\rm h}\boldsymbol{k}}^{\rm nr} = \Phi_{{\rm d}\boldsymbol{k}} \frac{4\pi G \rho_{\rm b}}{\sigma_{\rm h}^2} \frac{1}{k^2} \left\{1 + i\sqrt{\pi} \frac{k_y r_0\Omega_0 - \omega}{\sqrt{2}k\sigma_{\rm h}} \times {\rm erf}\left(i\frac{k_y r_0\Omega_0 - \omega}{\sqrt{2}k\sigma_{\rm h}}\right) \exp -\frac{(k_y r_0\Omega_0 - \omega)^2}{2k^2\sigma_{\rm h}^2}\right\}, \tag{25}$$

where the error function with imaginary argument is related to Dawson's integral. Since the gravitational forces in Eq. (1) have

to be taken at the midplane $z = 0$, it is necessary to convert $\Phi_{\mathrm{h}\boldsymbol{k}}$ from the representation in $\boldsymbol{k}$ space to a mixed representation in $(\boldsymbol{k}_\parallel, z)$ space leading to

$$\Phi^{\mathrm{nr}}_{\mathrm{h}\boldsymbol{k}_\parallel}(z=0) = \int_{-\infty}^{\infty} \mathrm{d}k_z \frac{k_\parallel}{(k_\parallel^2+k_z^2)^2} \Phi_{\mathrm{d}\boldsymbol{k}} \frac{4G\rho_{\mathrm{b}}}{\sigma_{\mathrm{h}}^2} \times\left\{1 + i\sqrt{\pi}\,\frac{k_y r_0\Omega_0-\omega}{\sqrt{2}k\sigma_{\mathrm{h}}}\,\mathrm{erf}\left(i\frac{k_y r_0\Omega_0-\omega}{\sqrt{2}k\sigma_{\mathrm{h}}}\right) \times\exp-\frac{(k_y r_0\Omega_0-\omega)^2}{2k^2\sigma_{\mathrm{h}}^2}\right\}. \quad (26)$$

The pole contribution to the integral in Eq. (24) has to be calculated according to Landau's rule resulting in

$$\Phi^{\mathrm{res}}_{\mathrm{h}\boldsymbol{k}} = \Phi_{\mathrm{d}\boldsymbol{k}} \frac{4\pi G\rho_{\mathrm{b}}}{\sigma_{\mathrm{h}}^2} \frac{1}{k^2} i\sqrt{\pi}\,\frac{k_y r_0\Omega_0-\omega}{\sqrt{2}k\sigma_{\mathrm{h}}} \times\exp-\frac{(k_y r_0\Omega_0-\omega)^2}{2k^2\sigma_{\mathrm{h}}^2} \quad (27)$$

and in the mixed representation

$$\Phi^{\mathrm{res}}_{\mathrm{h}\boldsymbol{k}_\parallel}(z=0) = -\int_{-\infty}^{\infty} \mathrm{d}k_z \frac{k_\parallel}{(k_\parallel^2+k_z^2)^2} \Phi_{\mathrm{d}\boldsymbol{k}} \frac{i}{\sqrt{\pi}} \frac{4\pi G\rho_{\mathrm{b}}}{\sigma_{\mathrm{h}}^2} \times\frac{\omega-k_y r_0\Omega_0}{\sqrt{2}k\sigma_{\mathrm{h}}}\,\exp-\frac{(k_y r_0\Omega_0-\omega)^2}{2k^2\sigma_{\mathrm{h}}^2}. \quad (28)$$

The final result can be formally written as

$$\Phi_{\mathrm{h}\boldsymbol{k}_\parallel}(z=0) = \Upsilon(\omega - k_y r_0\Omega_0, k_\parallel)\Phi_{\mathrm{d}\boldsymbol{k}_\parallel}, \quad (29)$$

where the real and imaginary parts of Υ are defined by Eqs. (26) and (28), respectively. Thus for any given frequency there is a contribution both from the non-resonant and the resonant halo particles. I find that in dimensionless form

$$\frac{(\omega-k_y r_0\Omega_0)^2}{2(k_\parallel^2+k_z^2)\sigma_{\mathrm{h}}^2} = 1.748\left(\frac{\sigma_{\mathrm{d}}}{\sigma_{\mathrm{h}}}\right)^2 \frac{1}{Q^2}\frac{k_{\mathrm{crit}}^2}{k_\parallel^2+k_z^2}\frac{(\omega-k_y r_0\Omega_0)^2}{\kappa^2}, \quad (30)$$

where σ_{d} denotes the velocity dispersion of the disk stars and $k_{\mathrm{crit}} = 2\pi/\lambda_{\mathrm{crit}}$ the critical wave number of the disk. The function Υ is illustrated in Fig. 1 for parameters typical for the solar neighbourhood in the Milky Way. The velocity dispersion of the halo particles has been estimated as $\sigma_{\mathrm{h}} = r_0\Omega_0/\sqrt{2}$ like in an isothermal sphere.

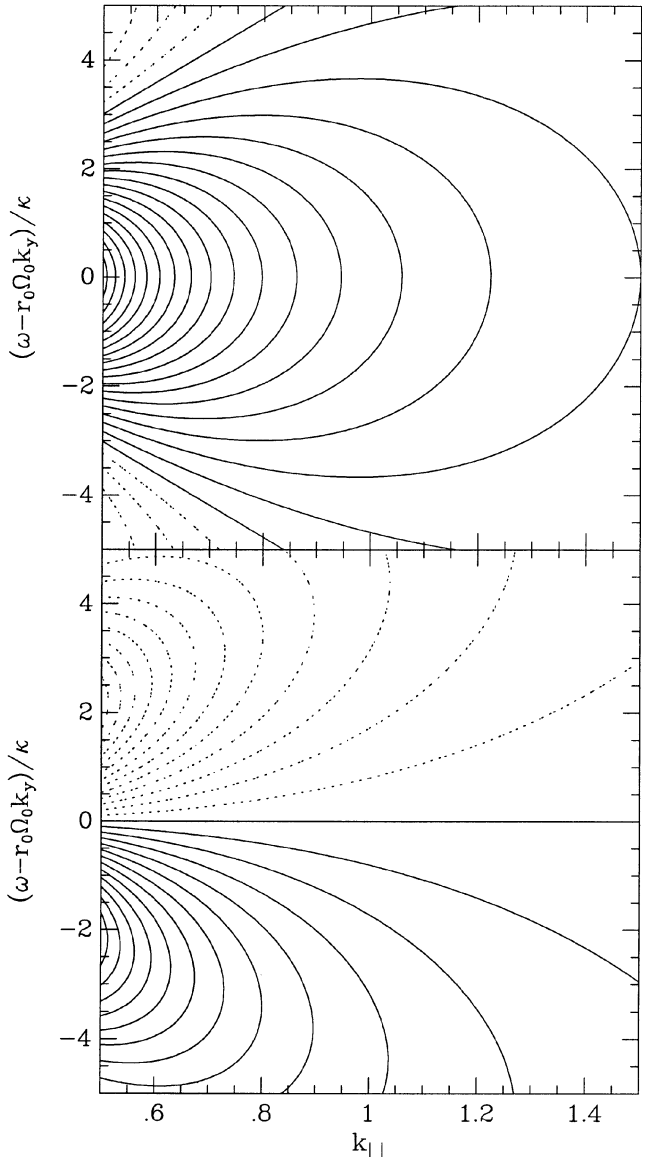

Fig. 1. The function $\Upsilon(\omega - k_y r_0\Omega_0, k_\parallel)$. The real part is shown in the upper panel, while the imaginary part is shown in the lower panel. The Doppler shifted frequency is given in terms of the epicyclic frequency and the wave number $k_\parallel$ in units of the critical wave number. Contours are given at levels of $10^{-2}G\rho_{\mathrm{b}}/\kappa^2$. Negative values are indicated as dotted lines. A Q parameter value of $Q = 1.4$ and a ratio of disk to halo velocity dispersions of σ_{d}:$\sigma_{\mathrm{h}} = 1$:5 are assumed.

4. Disk dynamics

The halo response (29) to the perturbation in the disk has to be inserted into Eq. (1). Solving the Boltzmann Eq. (1) is greatly facilitated by the fact that its form is identical to the case of an isolated shearing sheet with the replacement

$$\Phi_{\mathrm{d}\boldsymbol{k}} \to (1+\Upsilon)\Phi_{\mathrm{d}\boldsymbol{k}} \quad (31)$$

and I can use directly the results of Fuchs (2001) even though the Boltzmann equation is treated there using action and angle variables instead of the Cartesian coordinates as in Eq. (1). In particular the factor $1 + \Upsilon$ is carried straightforward through to the fundamental Volterra integral equation (Eq. (68) of Fuchs 2001)

$$\Phi_{\boldsymbol{k}',\omega} = \int_{-\infty}^{k_{\mathrm{x}}'} \mathrm{d}k_{\mathrm{x}}\mathcal{K}(k_{\mathrm{x}}, k_{\mathrm{x}}')\,(1+\Upsilon(k_x, k_y', \omega))\Phi_{\mathrm{k_x},\mathrm{k}_y',\omega} + r_{\boldsymbol{k}',\omega}, \quad (32)$$

where the kernel $\mathcal{K}$ is given by Eq. (67) of Fuchs (2001). $r_{\boldsymbol{k}'}$ describes an inhomogeneity of Eq. (32) related to an initial non-equilibrium state of the shearing sheet. Equation (32) is separating in the circumferential wave number k_y'. In Eq. (32) the wave numbers are expressed in units of the critical wave number k_{crit} (cf. Eq. (30)). This implies that the Volterra equation describing a shearing sheet embedded in a rigid halo potential is formally the same as that of an isolated shearing sheet,

because in this case $\Upsilon = 0$ and the halo mass affects only the numerical values of the critical wave number $k_{\rm crit}$ and the stability parameter Q. It is advantageous to consider Eq. (32) transformed back from frequency to time domain. Splitting off the ω-dependent term $\exp i\omega\frac{k_x-k'_x}{2Ak'_y}$ from the kernel and making use of the convolution theorem of the Fourier transform of products of two functions leads to

$$\Phi_{\boldsymbol{k}',\mathrm{t}} = \int_{-\infty}^{k'_\mathrm{x}} \mathrm{d}k_\mathrm{x}\tilde{\mathcal{K}}(k_\mathrm{x},k'_\mathrm{x}) \times\left\{\int_0^\infty \mathrm{d}t'\Phi_{\mathrm{k_x},\mathrm{k'_y},\mathrm{t'}}\delta\left(t-t'+\frac{k_x-k'_x}{2Ak'_y}\right) + \int_0^\infty \mathrm{d}t'\Phi_{\mathrm{k_x},\mathrm{k'_y},\mathrm{t'}}\mathcal{F}\left(\Upsilon(k_x,k'_y,\omega)\mathrm{e}^{i\omega\frac{k_x-k'_x}{2Ak'_y}}\right)_{\mathrm{t-t'}}\right\} + r_{\boldsymbol{k}',\mathrm{t}}, \quad (33)$$

where the operator $\mathcal{F}$ denotes the Fourier transform from ω to time domain. In Eq. (33) I have assumed an initial perturbation of the disk at time $t = 0$ so that $\Phi_{\mathrm{k_x},\mathrm{k'_y},t'<0} = 0$. The Fourier transform $\mathcal{F}$ can be calculated analytically using formulae 6.317[1] and 3.952, and the integrals with respect to k_z using formula 3.466 of Gradshteyn & Ryzhik (2000) leading to

$$\mathcal{F}\left(\Upsilon(k_x,k'_y,\omega)\mathrm{e}^{i\omega\frac{k_x-k'_x}{2Ak'_y}}\right)_{\mathrm{t-t'}} = \frac{4\pi^2G\rho_\mathrm{b}}{\sigma_\mathrm{h}^2}\frac{1}{k_\mathrm{x}^2+{k'_y}^2} \times\delta\left(t-t'+\frac{k_x-k'_x}{2Ak'_y}\right) + 4\pi^2G\rho_\mathrm{b} \times\exp\left[ik'_yr_0\Omega_0\left(t-t'+\frac{k_x-k'_x}{2Ak'_y}\right)\right] \times\left\{\left(t-t'+\frac{k_x-k'_x}{2Ak'_y}\right)+\left|t-t'+\frac{k_x-k'_x}{2Ak'_y}\right|\right\} \times\mathrm{erfc}\left(\frac{\sigma_\mathrm{h}}{\sqrt{2}}\sqrt{k_x^2+{k'_y}^2}\left|t-t'+\frac{k_x-k'_x}{2Ak'_y}\right|\right), \quad (34)$$

where the terms depending on the delta function and the absolute value $\left|t-t'+\frac{k_x-k'_x}{2Ak'_y}\right|$ in the curly bracket represent the contribution from the non-resonant halo particles, while the remaining term gives the contribution by the resonant halo particles. If this is inserted into Eq. (33) it takes the form

$$\Phi_{\boldsymbol{k}',\mathrm{t}} = \int_{-\infty}^{k'_\mathrm{x}} \mathrm{d}k_\mathrm{x}\tilde{\mathcal{K}}(k_\mathrm{x},k'_\mathrm{x})\left\{\Phi_{k_x,k'_y,t+\frac{k_x-k'_x}{2Ak'_y}} + \int_0^{t+\frac{k_x-k'_x}{2Ak'_y}}\mathrm{d}t'\Phi_{k_x,k'_y,t'} \times\mathcal{F}\left(\Upsilon(k_x,k'_y,\omega)\mathrm{e}^{i\omega\frac{k_x-k'_x}{2Ak'_y}}\right)_{\mathrm{t-t'}}\right\} + r_{\boldsymbol{k}',t}. \quad (35)$$

Equation (35) can be integrated numerically with very modest numerical effort. In Fig. 2 I illustrate the response of the shearing sheet now embedded in a live halo to an initial sinusoidal perturbation of unit amplitude. For this purpose I use the inhomogeneity term of the Volterra equation

$$r_{\boldsymbol{k}',\omega} = \int_{-\infty}^{k'_\mathrm{x}} \mathrm{d}k_\mathrm{x}\mathcal{L}(k_\mathrm{x},k'_\mathrm{x})\,f_{k_x,k'^{\mathrm{in}}_y}(0) \quad (36)$$

[1] I use the identity $\int_0^\infty \mathrm{d}\omega\cos(b\omega)a\omega\mathrm{erf}(ia\omega)\mathrm{e}^{-a^2\omega^2} = a\frac{\partial}{\partial b}\int_0^\infty \mathrm{d}\omega\sin(b\omega)\mathrm{erf}(ia\omega)\mathrm{e}^{-a^2\omega^2}$ with formula 6.317.

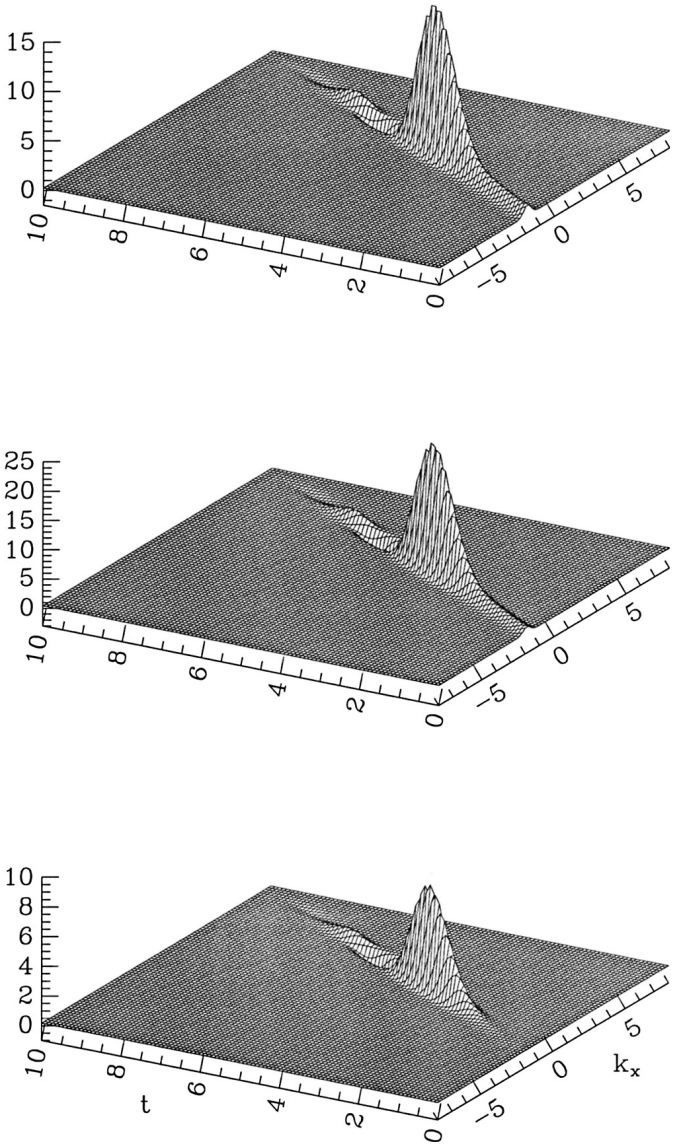

Fig. 2. Swing amplified density wave in the shearing sheet. The upper diagram shows the evolution in a shearing sheet embedded in a static halo potential triggered by an impulse with unit amplitude and wave vector $\boldsymbol{k}^{\rm in} = (-2, 0.5)k_{\rm crit}$. Time is given in units of 0.045 epicycle periods. The middle diagram shows the evolution of a shearing sheet embedded in a live dark halo triggered by the same impulse. The lower diagram shows the difference. The model parameters are $A/\Omega_0 = 0.5, Q = 1.4, \sigma_\mathrm{d}{:}\sigma_\mathrm{h} = 1{:}5, G\rho_\mathrm{b}/\kappa^2 = 0.01$, and $r_0\Omega_0{:}\sigma_\mathrm{d} = 220{:}44$.

derived in Fuchs (2001) with $f_{k_x,k'^{\mathrm{in}}_y}(0) \propto \delta(k_x - k_x^{\rm in})$. The response of the shearing sheet to this initial impulse is a swing amplification event. The radial wave number k_x evolves as

$$k_x = k_x^{\rm in} + 2Ak'^{\,\rm in}_y t, \quad (37)$$

while the circumferential wave number $k'^{\,\rm in}_y$ is constant, which means that the wave crests swing around from leading to trailing orientation during the amplification phase. Around $t = 6$ the amplitudes become negative which indicates that the swing amplified density wave is also oscillating. As can be seen from Fig. 2 comparing the evolution of shearing sheets embedded

either in a rigid halo potential or a live halo this characteristic behaviour of the density wave is not changed by the responsive halo, but the maximum growth factor of the amplitude of the wave is enhanced by a surprisingly large amount. In Fig. 2 the evolution of a shearing sheet embedded in a static halo potential has been calculated from Eq. (35) setting $\mathcal{F} = 0$. The maximum growth factor is identical to within 1% accuracy with the maximum growth factor calculated by Fuchs (2001) in an alternative way. To test the accuracy of the numerical solution of the full Eq. (35) I have increased the velocity dispersion of the halo particles to $\sigma_{\rm d}{:}\sigma_{\rm h} = 1{:}13$. The halo is then very stiff and the enhancement of the maximum growth factor of the amplitude of the wave by the responsive halo is only 5.3% so that the solution of Eq. (35) is very similar to that for a density wave in a shearing sheet in a static halo. If I use this, which is correctly calculated, in the second term of Eq. (35) I confirm by this iterated solution the maximum growth factor of the self-consistent solution of Eq. (35) to an accuracy better than 1%. The enhanced maximum growth factor of swing amplified density waves due to a responsive halo seems to be the equivalent of the enhanced growth of bars of stellar disks embedded in live dark halos seen in the numerical simulations. However, the interaction of the shearing sheet and the surrounding halo is not only mediated by the resonant halo particles, but the non-resonant halo particles play an important role as well. This can be demonstrated, for instance, by keeping in Eq. (34) only that part of the Υ function related to the resonant halo particles and solving Eq. (35) approximately by iterating the solution for the isolated sheet,

$$\Phi_{\boldsymbol{k}',\mathrm{t}} \approx \int_{-\infty}^{k'_{\mathrm{x}}} \mathrm{d}k_{\mathrm{x}} \tilde{\mathcal{K}}(k_{\mathrm{x}}, k'_{\mathrm{x}}) \left\{ \Phi_{k_x, k'_y, t+\frac{k_x - k'_x}{2Ak'_y}} + \int_0^{\infty} \mathrm{d}t' \Phi^{\mathrm{iso}}_{k_x, k'_y, t'} \mathcal{F} \left(\Upsilon^{\mathrm{res}}(k_x, k'_y, \omega) \mathrm{e}^{i\omega \frac{k_x - k'_x}{2Ak'_y}} \right)_{\mathrm{t-t'}} \right\} + r_{\boldsymbol{k}',t}. \quad (38)$$

The amplification of density waves depends critically on the Toomre stability parameter Q. This is illustrated in Fig. 3 where the response of the shearing sheet to the same initial impulse as in the previous example is shown, but assuming a stability parameter of $Q = 2$. As can be seen in Fig. 3 there is neither effective amplification of density waves in a shearing sheet in a rigid halo potential or in a shearing sheet embedded in a live dark halo.

In Fig. 4 I illustrate the maximum growth factors as function of the circumferential wave number k_y for shearing sheets embedded in a rigid halo potential or a live dark halo, respectively. As can be seen from Fig. 4 in both cases maximum amplification occurs for wave numbers around $k_y = 0.5$ or in the notation of Toomre (1981) $X = k_y^{-1} = 2$. Thus the preferred circumferential wave length of the density waves is $2\lambda_{\rm crit}$.

Following Athanassoula et al. (1987) arguments of swing amplification theory have been used to constrain the mass-to-light ratios of galactic disks. The expected number of spiral arms is determined by how often the azimuthal wave length $2\pi/k_y$ fits onto the circular annulus,

$$m = \frac{2\pi r_0}{\frac{2\pi}{k_y}}. \quad (39)$$

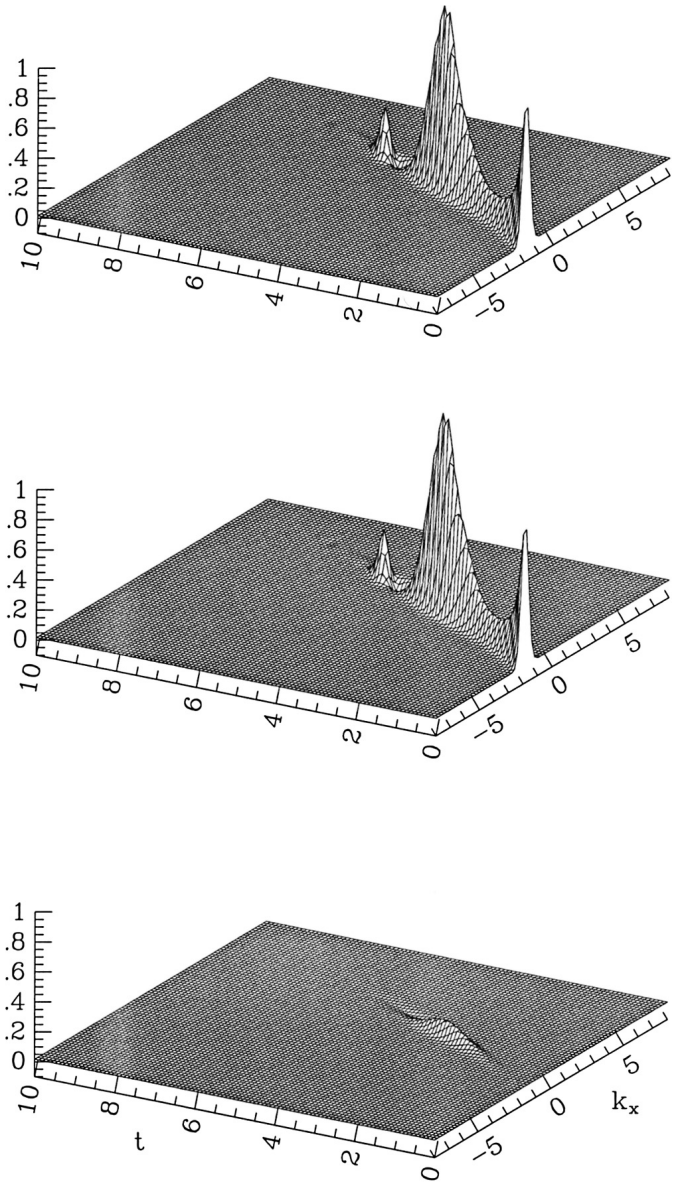

Fig. 3. Same as in Fig. 2, but adopting $Q = 2$.

As shown in Fig. 4 density waves grow preferentially with an azimuthal wave number around $k_y \approx 0.5 k_{\rm crit}$. This assumes a disk with a flat rotation curve, $A/\Omega_0 = 0.5$, but the preferred wave length varies with the slope of the rotation curve measured by Oort's constant A (cf. Fuchs 2001). The observed number of spiral arms of a galaxy taken together with the rotation curve allows then to determine the surface density of the disk. Since the wave number of maximum growth of the density wave amplitudes is the same for shearing sheets embedded either in a rigid halo potential or in a live dark halo, the presence of a responsive dark halo does not influence the constraints on the disk mass obtained this way.

Another constraint on the disk mass depends on the implied value of the Toomre stability parameter Q (Fuchs 1999, 2003). Q must be larger than $Q = 1$ in order to avoid Jeans like instabilities in the disks (Toomre 1964). A disk violating this condition will evolve rapidly by fierce dynamical instabilities above the threshold of $Q = 1$ (Fuchs & von Linden 1998).

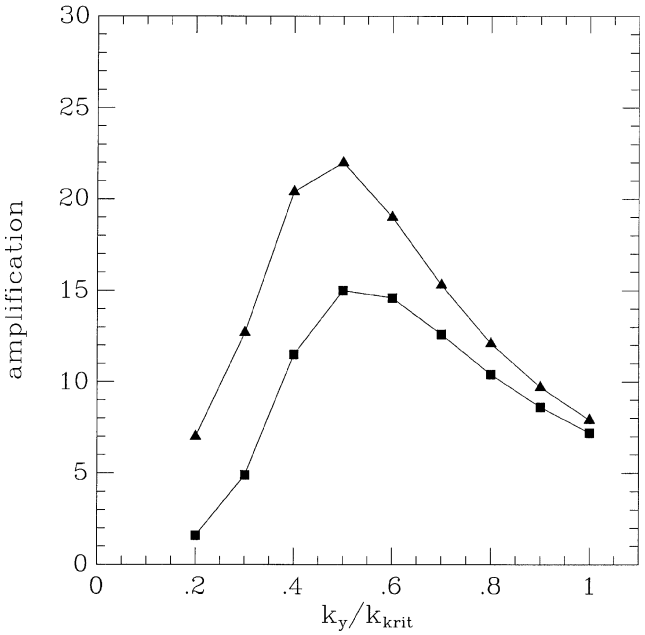

Fig. 4. Maximum growth factors of swing amplified density waves in a shearing sheet embedded in a rigid halo potential (squares) and in a shearing sheet embedded in a live dark halo (triangles). The same model parameters as above have been adopted.

On the other hand, I have demonstrated above that the Q value must be less than $Q = 2$ in order that the disk can develop appreciable spiral structure. If the radial velocity dispersions of the stars are known, the allowed range of Q sets constraints on the disk mass, which are independent from the previous ones (cf. Eqs. (6) and (7)). As shown in Fig. 3 this condition is not changed by the presence of a live dark halo.

5. Momentum transfer to the halo

The analogue of the angular momentum transfer from bars to dark halos is in the shearing sheet the transfer of linear momentum to the surrounding halo particles. In order to describe this I adapt the discussion of Dekker (1976) to the shearing sheet model. The acceleration of a halo particle is given by

$$\dot{\boldsymbol{v}} = -\nabla\Phi, \tag{40}$$

where I assume a gravitational potential of the form

$$\Phi(\boldsymbol{x}, t) = \Re\{\Phi(\boldsymbol{x})\mathrm{e}^{i\omega t}\}, \tag{41}$$

with complex frequency ω. Thus the overall acceleration of the halo is given by

$$\langle\dot{\boldsymbol{v}}\rangle = -\int \mathrm{d}^3x \int \mathrm{d}^3v f_\mathrm{h} \nabla\Phi. \tag{42}$$

If both the gravitational potential and the distribution function of the halo particles are Fourier expanded[2],

$$\begin{aligned}\langle\dot{\boldsymbol{v}}\rangle &= -\int \mathrm{d}^3x \int \mathrm{d}^3v \int \mathrm{d}^3k\, i\boldsymbol{k}\Phi_{\boldsymbol{k}}(t)\mathrm{e}^{i(\boldsymbol{k},\boldsymbol{x})} \\ &\quad\times \int \mathrm{d}^3k' f_{\mathrm{h}\boldsymbol{k}'}(t)\mathrm{e}^{i(\boldsymbol{k}',\boldsymbol{x})} \\ &= (2\pi)^3 \int \mathrm{d}^3v \int \mathrm{d}^3k\, i\boldsymbol{k}\Phi_{-\boldsymbol{k}}(t) f_{\mathrm{h}\boldsymbol{k}}(t).\end{aligned} \tag{43}$$

In order that the gravitational potential Φ be a real quantity its Fourier coefficients must obey the relation $\Phi_{-\boldsymbol{k}}(t) = \Phi^*_{\boldsymbol{k}}(t)$, and for a potential of the form (41) one can write

$$\Phi_{\boldsymbol{k}}(t) = \frac{1}{2}\left\{\Phi_{\boldsymbol{k}}\mathrm{e}^{i\omega t} + \Phi^*_{-\boldsymbol{k}}\mathrm{e}^{-i\omega^* t}\right\}. \tag{44}$$

Again spatial coordinates ξ, η, and ζ are introduced with the ξ-axis parallel to the wave vector $\boldsymbol{k}$ and using Eq. (11) one obtains from Eq. (43)

$$\begin{aligned}\langle\dot{\upsilon}\rangle &= i(2\pi)^3 \int \mathrm{d}^3k \int_{-\infty}^{\infty} \mathrm{d}\upsilon \frac{\rho_\mathrm{b}}{\sqrt{2\pi}\sigma_\mathrm{h}^3} \mathrm{e}^{-\frac{\upsilon^2}{2\sigma_\mathrm{h}^2}} \\ &\quad\times\frac{k}{4}\left\{\Phi_{-\boldsymbol{k}}\mathrm{e}^{i\omega t} + \Phi^*_{\boldsymbol{k}}\mathrm{e}^{-i\omega^* t}\right\} \\ &\quad\times\left\{-k\Phi_{\boldsymbol{k}}\frac{\upsilon\mathrm{e}^{i\omega t}}{\omega + k\upsilon} - k\Phi^*_{-\boldsymbol{k}}\frac{\upsilon\mathrm{e}^{-i\omega^* t}}{-\omega^* + k\upsilon}\right\}.\end{aligned} \tag{45}$$

In Eq. (45) I have integrated already over the velocity components perpendicular to the ξ-axis. Two of the four terms of the integrand cancel out leading to

$$\begin{aligned}\langle\dot{\upsilon}\rangle &= -2\pi^3 i \int \mathrm{d}^3k \int_{-\infty}^{\infty} \mathrm{d}\upsilon \frac{\rho_\mathrm{b}}{\sqrt{2\pi}\sigma_\mathrm{h}^3} \mathrm{e}^{-\frac{\upsilon^2}{2\sigma_\mathrm{h}^2}} \\ &\quad\times k^2\mathrm{e}^{-2\Im\omega t}|\Phi_{\boldsymbol{k}}|^2\left\{\frac{\upsilon}{\omega + k\upsilon} - \frac{\upsilon}{\omega^* + k\upsilon}\right\}.\end{aligned} \tag{46}$$

In the limit of $-\Im\omega \to 0$

$$\frac{\upsilon}{\omega + k\upsilon} - \frac{\upsilon}{\omega^* + k\upsilon} \to -i2\pi\upsilon\delta(\Re\omega + k\upsilon), \tag{47}$$

and I find

$$\begin{aligned}\langle\dot{\upsilon}\rangle &= -4\pi^4 \int \mathrm{d}^3k \frac{\rho_\mathrm{b}}{\sqrt{2\pi}\sigma_\mathrm{h}^3}|\Phi_{\boldsymbol{k}}|^2(\omega - k_y r_0\Omega_0) \\ &\quad\times\exp -\frac{(\omega - k_y r_0\Omega_0)^2}{2k^2\sigma_\mathrm{h}^2},\end{aligned} \tag{48}$$

where ω denotes now the frequency of the wave in the reference frame of the shearing sheet as in the previous sections. Note that according to the notation used here $(\omega - k_y r_0\Omega_0) < 0$ for waves traveling along the y-axis in the forward direction, so that $\langle\dot{\upsilon}\rangle > 0$ for such waves. From the form of the Fourier coefficients (18) it becomes immediately clear that only planar momentum is transferred to the halo, $\langle\dot{v}_z\rangle = 0$, as expected from symmetry reasons. $\langle\dot{v}_x\rangle$ and $\langle\dot{v}_y\rangle$ depend on the exact form

[2] It can be shown (Binney & Tremaine 1987 and references therein) that if the Fourier transformed potential of a point mass is inserted into Eq. (43) this leads exactly to Chandrasekhar's dynamical friction formula, although with a Coulomb logarithm defined in a slightly different way.

of the power spectrum $|\Phi_k|^2$. Equation (47) shows that linear momentum transfer to the halo is mediated entirely by halo particles on orbits resonant with the wave. This is exactly the same as for angular momentum transfer from bars to halos (Weinberg 1985; Weinberg & Katz 2000; Athanassoula 2003; Sellwood 2003). It has also been known for a long time for the angular momentum exchange between spiral density waves and galactic disks (Lynden-Bell & Kalnajs 1972) or for momentum transfer from longitudinal plasma waves (Stix 1962). It is interesting that the exchanged linear momentum scales as ρ_b/σ_h^3 in Eq. (48). This implies that at given mass a dynamical hot halo absorbs less momentum than a cooler one. On the other hand, the shearing sheet would loose less momentum. The same effect has been described by Athanassoula (2003) for the angular momentum transfer from bars to halos.

6. Summary and conclusions

If a self-gravitating shearing sheet is embedded in a live dark halo, the halo particles respond unexpectedly strongly to density waves in the sheet. The interaction between the density waves and the halo particles is mediated both by halo particles on orbits in resonance with the waves and on non-resonant orbits. If the embedded shearing sheet is initially perturbed by a sinusoidal wave, a swing amplified density wave develops in the disk, which is of the same type as in an isolated sheet or a sheet in a static halo potential, but with an amplitude enhanced by a surprisingly large amount. This appears to be the equivalent of the enhanced bar growth in stellar disks embedded in live dark halos instead of static halo potentials seen in numerical simulations. There is transfer of linear momentum of density waves in the shearing sheet to the halo particles. However, this is mediated, entirely by halo particles on orbits in resonance with the waves similar to the torque exerted by bars on the surrounding halo.

Acknowledgements. I thank E. Athanassoula for stimulating discussions and the anonymous referee for helpful comments.

References

Athanssoula, E. 2002, ApJ, 569, L83
Athanssoula, E. 2003, MNRAS, 341, 1179
Athanssoula, E., Bosma, A., & Papaioannou, S. 1987, A&A, 179, 23
Binney, J., & Tremaine, S. 1987, Galactic Dynamics (Princeton: Princeton Univ. Press), 487
Debattista, V. P., & Sellwood, J. A. 2000, ApJ, 543, 704
Dekker, E. 1976, Phys. Rep., 24, 315
Fuchs, B. 1999, ASP Conf. Ser., 182, 365
Fuchs, B. 2001, A&A, 368, 107
Fuchs, B. 2003, in Proc. Fourth Int. Workshop on the Identification of Dark Matter, ed. N. J. C. Spooner, & V. Kudryavtsev (Singapore: World Scientific), 72
Fuchs, B. 2004, A&A, submitted
Fuchs, B., & von Linden, S. 1998, MNRAS, 294, 513
Goldreich, P., & Lynden-Bell, D. 1965, MNRAS, 130, 125
Gradshteyn, I. S., & Ryzhik, I. M. 2000, Table of Integrals, Series, and Products, 6th Ed. (New York: Academic Press)
Julian, W. H., & Toomre, A. 1966, ApJ, 146, 810
Kegel, W. H. 1998, Plasmaphysik (Berlin: Springer)
Lynden-Bell, D., & Kalnajs, A. J. 1972, MNRAS, 157, 1
Ostriker, J. P., & Peebles, P. J. E. 1973, ApJ, 186, 467
Sellwood, J. A. 2003, ApJ, 587, 638
Stix, T. H. 1962, The theory of plasma waves (New York: McGraw-Hill)
Toomre, A. 1964, ApJ, 139, 1217
Toomre, A. 1977, ARA&A, 15, 437
Toomre, A. 1981, in The Structure and Evolution of Normal Galaxies, ed. S. M. Fall, & D. Lynden-Bell (Cambridge: Cambridge Univ. Press), 111
Weinberg, M. D. 1985, MNRAS, 213, 451
Weinberg, M. D., & Katz, N. 2002, ApJ, 580, 627